





Article

Attachment and Growth of Fibroblast Cells on Poly (2-Methoxyethyl Acrylate) Analog Polymers as Coating Materials

Rubaiya Anjum ^{1,†} , Kei Nishida ^{2,†} , Haruka Matsumoto ¹, Daiki Murakami ^{1,2} , Shingo Kobayashi ², Takahisa Anada ^{1,2,*} and Masaru Tanaka ^{1,2,*} 

- ¹ Department of Chemistry and Biochemistry, Graduate School of Engineering, 744 Motooka, Nishi-ku, Fukuoka 819-0395, Japan; anjum.rubaiya.867@s.kyushu-u.ac.jp (R.A.); matsumoto.haruka.093@s.kyushu-u.ac.jp (H.M.); daiki_murakami@ms.ifoc.kyushu-u.ac.jp (D.M.)
- ² Institute for Materials Chemistry and Engineering, Kyushu University, 744 Motooka, Nishi-ku, Fukuoka 819-0395, Japan; kei_nishida@ms.ifoc.kyushu-u.ac.jp (K.N.); shingo_kobayashi@ms.ifoc.kyushu-u.ac.jp (S.K.)
- * Correspondence: takahisa_anada@ms.ifoc.kyushu-u.ac.jp (T.A.); masaru_tanaka@ms.ifoc.kyushu-u.ac.jp (M.T.); Tel./Fax: +81-92-802-6238 (T.A. & M.T.)
- † These authors contributed equally to this work.



Citation: Anjum, R.; Nishida, K.; Matsumoto, H.; Murakami, D.; Kobayashi, S.; Anada, T.; Tanaka, M. Attachment and Growth of Fibroblast Cells on Poly (2-Methoxyethyl Acrylate) Analog Polymers as Coating Materials. *Coatings* **2021**, *11*, 461. <https://doi.org/10.3390/coatings11040461>

Academic Editor: Roman A. Surmenev

Received: 10 March 2021
Accepted: 14 April 2021
Published: 16 April 2021

Publisher's Note: MDPI stays neutral with regard to jurisdictional claims in published maps and institutional affiliations.



Copyright: © 2021 by the authors. Licensee MDPI, Basel, Switzerland. This article is an open access article distributed under the terms and conditions of the Creative Commons Attribution (CC BY) license (<https://creativecommons.org/licenses/by/4.0/>).

Abstract: The regulation of adhesion and the subsequent behavior of fibroblast cells on the surface of biomaterials is important for successful tissue regeneration and wound healing by implanted biomaterials. We have synthesized poly(ω -methoxyalkyl acrylate)s (PMCA_xs; x indicates the number of methylene carbons between the ester and ethyl oxygen), with a carbon chain length of $x = 2-6$, to investigate the regulation of fibroblast cell behavior including adhesion, proliferation, migration, differentiation and collagen production. We found that PMC2A suppressed the cell spreading, protein adsorption, formation of focal adhesion, and differentiation of normal human dermal fibroblasts, while PMC4A surfaces enhanced them compared to other PMCA_xs. Our findings suggest that fibroblast activities attached to the PMCA_x substrates can be modified by changing the number of methylene carbons in the side chains of the polymers. These results indicate that PMCA_xs could be useful coating materials for use in skin regeneration and wound dressing applications.

Keywords: PMEA analog polymers; coating materials; fibroblasts; cell behavior; wound dressing

1. Introduction

Coatings on implanted biomaterials play a pivotal role in regulating biological reactions after implantation [1,2]. Various coating approaches such as covalent and physically adsorbed coating have been developed to reduce biological reaction and improve biocompatibility [3,4]. To ensure biocompatibility, it is critical to control the contact between the biomaterial surface and biological components, including proteins and cells [5]. Cell adhesion and growth on biomaterials are indicators of biocompatibility, as these behaviors are involved in the adsorbed biological components and biological response on the surface of the biomaterial [6,7]. Therefore, in order to develop better biomaterials, it is necessary to understand the regulation of cell adhesion and its subsequent behavior on the implant surface. The selection of a suitable surface for the implanted biomaterials is also an important issue from the perspective of cell–material interactions. The interactions between the surface of biomaterials and cells are responsible for regulating cell fate and tissue regeneration.

Fibroblasts play an important role in tissue remodeling and wound healing [8,9]. Because their functions are related to the epidermal proliferation, differentiation, and formation of extracellular matrix (ECM), fibroblast regulation is linked to the integration or disintegration of biomaterials in tissue engineering and wound healing [8]. In the

regeneration of functional tissues, extracellular signals occasionally convert a quiescent state of fibroblasts into an active phenotype known as myofibroblasts, which are required for inducing tissue connection and contraction [10,11]. Myofibroblasts create a type of environment/network during tissue regeneration that results in cell differentiation, proliferation, quiescence, and apoptosis. In the case of natural healing processes, they release an excess amount of matrix proteins to promote faster healing. However, the over and prolonged activation of myofibroblasts induces the formation of fibrotic tissues [12–14]. This promotes the development of numerous diseases and plays a major role in most organ failure cases. Therefore, it is important to regulate the balance between fibroblast recruitment and differentiation on the surface of implanted biomaterials.

Several groups have demonstrated that fibroblast behavior is controlled by modulating surface properties, including wettability, roughness, elasticity, micro and nanostructure, polarity, and hydrophobicity [6,15–17]. These properties contribute to altering the signal transduction via focal adhesion signaling, which is responsible for the dynamic relationship between the integrins of cells adhered on surfaces and adhesive proteins, including fibronectin (FN) and vitronectin [7,18,19]. In this regard, the surface properties, including cell adhesiveness on the biomaterials, can be modified by a polymer coating on the surface [20–22]. Therefore, the use of synthetic polymeric coatings on implanted biomaterials can be a suitable approach for controlling cellular behavior. Our group has developed a biocompatible poly(2-methoxyethyl acrylate) (PMEA) and its analogs as coating materials that exhibit excellent non-thrombogenicity and selective cell adhesivity [23–25]. In addition, the mechanism underlying these properties is related to the hydrated water on the PMEA analogs. Hydrated water can be classified into three types: non-freezing water (NFW), intermediate water (IW), and free water, based on the mode of binding defined by time-resolved infrared spectroscopy, nuclear magnetic resonance relaxation time, and differential scanning calorimetry (DSC) [26–28]. In particular, PMEA analogs modulate protein adsorption and conformational changes on the surface according to the IW content [29–31]. Furthermore, PMEA analogs promote the adipogenesis of mouse adipocyte precursor cells by suppressing the conformational change of adsorbed proteins and subsequent integrin signaling [32]. These results indicate that PMEA analogs can modulate the amount and conformation of the adsorbed protein, thereby regulating cellular behavior. Thus, we hypothesized that PMEA analogs could be used as coating materials on biomaterials to regulate fibroblast behavior, including adhesion, recruitment, and differentiation. However, the relationship between fibroblast behavior and PMEA analogs with varying hydration water contents has yet to be clarified.

Poly(ω -methoxyalkyl acrylate) (PMC x As; where x indicates the number of methylene carbons between the ester and ethyl oxygen) has been reported to be a PMEA analog polymer that can systemically modulate hydrophobicity, hydration water content, and protein adsorption [33]. Thus, we anticipated that PMC x As with changes in carbon chain length would modulate fibroblast behavior. Here, we evaluated fibroblast behavior, including adhesion, migration, differentiation, and collagen secretion, on PMC x As. PMC x As were developed as coating materials to regulate fibroblast behavior. Therefore, we examined the attachment and growth of normal human dermal fibroblasts (NHDFs) on PMC x A-coated substrates. To estimate the focal adhesion signaling activity, the formation of focal adhesions and the amount of adsorbed FN were evaluated. Moreover, the expression of specific proteins, cell migration, and collagen production were assessed to determine the activation of NHDFs in response to the PMC x A properties.

2. Materials and Methods

2.1. Preparation of Polymer-Coated Substrates

Poly(2-methoxyethyl acrylate) (PMC2A), poly(3-methoxypropyl acrylate) (PMC3A), poly(4-methoxybutyl acrylate) (PMC4A), poly(5-methoxypentyl acrylate) (PMC5A), and poly(6-methoxyhexyl acrylate) (PMC6A) were synthesized as described previously [33], and their chemical structures are represented in Figure 1. The toluene solutions (0.5 wt.%/vol.%) of each

polymer were used to prepare the polymer substrates. Each polymer was spin-coated on a polyethylene terephthalate (PET) disc (thickness = 125 μm) (Mitsubishi Plastics, Tokyo, Japan) of 14 and 30 mm in diameter at 3000 rpm for 40 s. Then, the polymer-coated substrates were dried and stored in a desiccator. Prior to each experiment, the prepared substrate was sterilized by exposure to UV for 1 h.

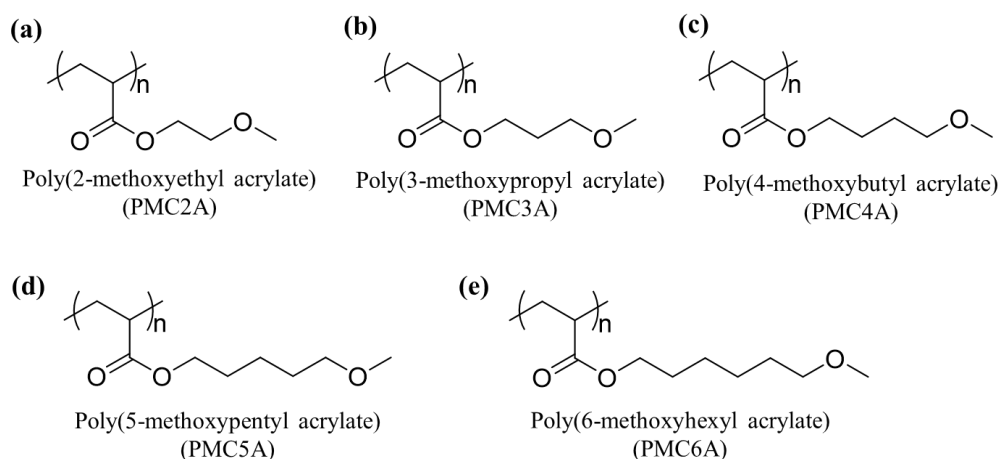


Figure 1. Chemical structures of poly(ω -methoxyalkyl acrylates) (PMCA_xAs): (a) poly(2-methoxyethyl acrylate) (PMC2A); (b) poly(3-methoxypropyl acrylate) (PMC3A); (c) poly(4-methoxybutyl acrylate) (PMC4A); (d) poly(5-methoxypentyl acrylate) (PMC5A); (e) poly(6-methoxyhexyl acrylate) (PMC6A).

2.2. Contact Angle Measurement

The contact angles of each prepared polymer substrate were measured using two techniques: sessile water droplet and captive air bubble. The droplet method was executed by placing 2 μL of water droplets on the five positions of the substrate. For captive bubble measurement, the prepared polymer substrates were immersed in water for 24 h. Then, 2 μL of air bubbles were injected at the three positions beneath the substrate.

2.3. Cell Culture

NHDFs (Lonza, Warsaw, Poland) were cultured in a media consisting of Dulbecco's modified Eagle's medium/nutrient mixture (DMEM/F12) (1:1), 10% (v/v) fetal bovine serum, and 1% (v/v) penicillin-streptomycin (all from Thermo Fisher Scientific, Waltham, MA, USA). Prior to the experiment, cells were isolated from the culture dish using 0.25% trypsin/EDTA solution (Thermo Fisher Scientific, Rockford, IL, USA).

2.4. Cell Attachment and Proliferation Assays

Cell proliferation assays were performed using 24-well plates. For the proliferation assay, NHDFs were cultured on each PMCA_xA-coated PET substrate ($\varphi = 14$ mm) at a density of 5×10^3 cells/ cm^2 for 24, 96, and 168 h. All substrates were pre-soaked in phosphate-buffered saline (PBS) (–) and incubated for 1 h at 37 $^\circ\text{C}$ prior to cell seeding. After the specified incubation time, the number of cells was determined from a standard curve prepared using the colorimetric WST-8 assay (Dojindo Laboratories, Kumamoto, Japan). The calcein reagent (Thermo Fisher Scientific, Rockford, IL, USA) was used to stain living cells after 24 h of cultivation. Fluorescence images were captured to observe living cells.

2.5. Quantification of Adsorbed Protein on Polymer Substrates

The amount of total adhered proteins was measured by performing a bicinchoninic acid assay with the micro-BCA protein assay kit (Thermo Fisher Scientific, Rockford, IL, USA) according to the manufacturer's instructions. All polymer substrates with a diameter of 30 mm were used in this experiment. First, the substrates were pre-soaked in PBS (–) for

1 h at room temperature. Then, protein solution (10 µg/mL in PBS (–)) was added to each well and incubated for 1 h at 37 °C. After protein adsorption, the substrates were rinsed three times with PBS. Next, 5% (*w/v*) sodium dodecyl sulfate (SDS) (Bio-Rad Laboratories, Tokyo, Japan) and 0.1 M NaOH solutions were added to 6-well plates and incubated at 37 °C for 2 h. The surface of the substrate was scratched using a cell scraper to peel off the adsorbed protein from the substrate. Finally, the extracted protein solution was mixed with BCA solution to measure the absorbance at a wavelength of 562 nm. The amount of adsorbed protein was calculated using the standard curve.

2.6. Immunocytochemical Analysis

Before starting the experiment, the prepared substrates were pretreated with PBS, following cell attachment and proliferation assays. NHDFs (1×10^4 cells/cm²) were seeded on each PMCA-coated substrate ($\varphi = 14$ mm) and incubated for 24 h. After culturing, the cells were fixed using 4% (*w/v*) paraformaldehyde (Fujifilm Wako Pure Chemical Corporation, Osaka, Japan) and incubated at 37 °C for 10 min. Then, 0.5% (*v/v*) Triton X-100 (Fujifilm Wako Pure Chemicals Co., Ltd., Osaka, Japan) in PBS (–) was added to permeabilize the cell membranes. The substrates were then treated with mouse monoclonal anti-human vinculin antibody (VIN-11-5; Sigma-Aldrich, St. Louis, MO, USA) (1:400) diluted in 1% (*w/v*) BSA dissolved in PBS (–) for 90 min at room temperature, and subsequently treated with Alexa Fluor 488-conjugated anti-mouse IgG (H + L) antibody (1:1000 dilution), Alexa Fluor 568-conjugated phalloidin (1:100 diluted), and 4',6-diamidino-2-phenylindole (1:1000 diluted) (all from Thermo Fisher Scientific, Waltham, MA, USA) for 1 h at room temperature. After performing these steps, the fluorescence images were captured using a confocal laser-scanning microscope (CLSM) (FV-1000; Olympus, Tokyo, Japan). Cell area and circularity were evaluated quantitatively using ImageJ software (version 1.53C, Bethesda, MD, USA).

2.7. Western Blotting

NHDFs (1×10^4 cells/cm²) were cultured on PMCA substrates ($\varphi = 30$ mm) for 24 h. The cells were washed twice with PBS and lysed with RIPA buffer (Fujifilm Wako Pure Chemical Corporation, Osaka, Japan) containing phosphatase (Nacalai Tesque, Kyoto, Japan) and protease inhibitors (Nacalai Tesque, Kyoto, Japan). The collected cell lysate was centrifuged at 12,000 rpm for 10 min at 4 °C. The supernatant was mixed with Laemmli buffer (Bio-Rad) containing 10% 2-mercaptoethanol and incubated at 95 °C for 3 min. For the collected solution, SDS-polyacrylamide gel electrophoresis (SDS-PAGE) was performed on a 4–20% gradient polyacrylamide gel (Bio-Rad, Hercules, CA, USA) for 50 min at 150 V. The separated proteins on the gels were transferred onto a polyvinylidene fluoride membrane (Bio-Rad, Hercules, CA, USA) using a Trans-Blot turbo transfer system (Bio-Rad, Hercules, CA, USA). The protein-transferred membrane was blocked with 5% skim milk or 5% BSA dissolved in TBS-T (20 mM Tris-HCl, 500 mM NaCl, 0.1% Tween-20, pH 7.5) for 60 min at room temperature. The primary antibodies were diluted with 5% skim milk or 3% BSA dissolved in TBS-T, added to the membrane, and incubated at 4 °C overnight. Rabbit monoclonal anti-Snail antibody (C15D3; Cell Signaling Technology, Tokyo, Japan) (1:1000 dilution), rabbit monoclonal anti- α -SMA antibody (E184; Abcam, Cambridge, UK) (1:1000 dilution), mouse monoclonal anti-vimentin antibody (10366-1-AP; Proteintech, Rosemont, IL, USA) (1:2000 dilution), and mouse monoclonal anti- β -actin antibody (6D1; MBL, Tokyo, Japan) (1:1000 dilution) were used as primary antibodies. Next, the membrane was washed with TBS-T and treated with horseradish peroxidase (HRP)-conjugated goat anti-mouse IgG (MBL, Tokyo, Japan) (1:10,000 dilution) or HRP-conjugated goat anti-rabbit IgG (MBL, Tokyo, Japan) (1:10,000 dilution) for 60 min at room temperature. The membrane was then washed with TBS-T and treated with ImmunoStar Zeta (Wako, Tokyo, Japan). Chemiluminescence images of the membrane were acquired using LuminoGraphI (WSE-6100; ATTO, Amherst, NY, USA). The band intensity of the captured images was measured using ImageJ software (version 1.53C, Bethesda, MD, USA).

2.8. Cell Migration Test

Cell migration experiments were performed in 6-well plates. First, NHDFs were cultured on PMCxA-coated substrates ($\varphi = 30$ mm) at 1×10^4 cells/cm² in 6-well plates and incubated at 37 °C. Then, the cell monolayer surface was scratched using a rubber cell scraper. Finally, cell migration was observed at 0, 24, and 48 h after the scratch and the images were captured using a phase-contrast microscope. The migration area was determined using Image J software and estimated as $(A_0 - A_t)$, where A_0 is the initial wound area and A_t is the wound area at the desired time (t). Then, the migration area was plotted against migration time, and finally, the rate of migration was calculated from the slope of this curve as $\text{slope}/2l$, where l is the length of the wounded region [34].

2.9. Collagen Production Measurement

NHDFs-secreted collagen was quantified using a collagen assay kit. For this experiment, the cells were seeded at a density of 2×10^4 cells/cm². L (+)-ascorbic acid sodium salt (1 mM) (Fujifilm Wako Pure Chemical Corporation, Osaka, Japan) was added as a supplement after 24 h of incubation at 37 °C to increase collagen production [35,36]. The media were collected after 7 days of cell culturing with supplements. The amount of collagen was normalized to the DNA concentration, as determined by the Picogreen assay (Thermo Fisher Scientific, Rockford, IL, USA).

2.10. Statistical Analysis

Data from at least three separate tests are presented as the mean \pm standard deviation (SD). Significance tests were performed using one-way analysis of variance (ANOVA) followed by Tukey's post hoc test for multiple comparisons. Statistical significance was set at $p < 0.05$.

3. Results and Discussion

3.1. Physicochemical Properties of PMCxA-Coated Substrates

Poly(ω -methoxyalkyl acrylate)s (PMCxAs; where x indicates the number of methylene carbons between the ester and ether oxygen) was synthesized following a previously reported method [33]. PMCxAs with a carbon chain length of $x = 2$ –6 were used. PMC2A has the same chemical structure as PMEAs. As per the previous report, the physicochemical properties, including molecular weight (M_n), glass transition temperature (T_g), IW content, and NFW content, were determined (Table 1). T_g , the transition temperature of the polymer from the glassy state to the rubbery state, is ascribed to the mobility of the polymer chain [37]. T_g decreased with an increasing length of the alkyl side chain under both dry and wet conditions, suggesting that the mobility of the polymer chains increased with the length of the alkyl side chain. Under wet conditions, the T_g values of PMCxAs were lower than those under dry conditions. The values of T_g decreased in the following order: PMC2A > PMC3A > PMC4A > PMC5A > PMC6A. Because the hydration of the polymer influences T_g , we calculated the hydration water content, such as IW and NFW, in PMCxAs [33]. The hydration water content of PMCxAs showed a steady decrease in the amount of IW along with the amount of NFW upon the introduction of the hydrophobic methylene carbon in the side chain.

To evaluate the cell adhesion behavior on PMCxAs, PMCxA-coated PET substrates were fabricated using spin-coating methods. Because the hydrophilicity on the surface is one of the parameters to modulate cell behavior, PMCxA-coated substrates were characterized by evaluating the contact angle to determine the hydrophilicity on the surface (Table 2). The contact angle values derived from each polymer-coated substrate were distinct from those of the uncoated PET substrate (86.4° in air and 129.2° in water), indicating that every polymer was coated properly. In the case of the sessile drop technique, the water contact angle increased with an increasing side chain alkyl length, suggesting that the hydrophilicity of polymers decreased with increasing side chain alkyl length. The contact angle values obtained with the captive air bubble method showed similar tendencies as the

sessile water drop, indicating that the hydrophilicity of the hydrated PMCxAs was similar before hydration. Therefore, the physicochemical properties of the PMCxAs showed that the side chain length affected the properties of the polymers.

Table 1. Physicochemical and thermal properties of PMCxAs [33] Copyright © 2017, American Chemical Society.

Scheme	M_n (kg/mol)	M_w/M_n	$T_{g \text{ dry}}^a$ (°C)	$T_{g \text{ wet}}^a$ (°C)	IW ^b (wt.%)	NFW ^c (wt.%)
PMC2A	32	1.3	−35	−51	3.7	2.5
PMC3A	33	2.7	−48	−58	2.8	3.1
PMC4A	24	2.4	−65	−67	1.7	1.3
PMC5A	31	2.8	−74	−78	1.0	1.5
PMC6A	42	2.7	−77	−78	0.8	1.3

^a Measured by DSC performed at a rate of 5 °C/min, ^b intermediate water (IW), and ^c non-freezing water (NFW).

Table 2. Contact angle of PET substrate coated with PMCxAs. The data represent the mean ± SD ($n = 5$).

Samples	Contact Angle (°)	
	Sessile Water Drops ^a	Captive Air Bubble ^a
PET	86.4 (± 1.1)	129.2 (± 1.0)
PMC2A	44.2 (± 0.6)	133.6 (± 1.0)
PMC3A	51.1 (± 0.4)	129.5 (± 1.7)
PMC4A	54.4 (± 0.7)	125.7 (± 1.7)
PMC5A	57.3 (± 0.2)	120.3 (± 0.6)
PMC6A	61.0 (± 0.6)	119.4 (± 3.7)

^a Sessile water drops method by placing a 2 µL water droplet for 30 s and a captive air bubble method by placing 2 µL air bubble on the substrates immersed in water for 24 h.

3.2. Cell Attachment and Proliferation Assay

In the field of designing and improving biomaterials, the capacity for cell attachment is considered an important factor. The physicochemical properties of the surface affect the behavior of adhered cells on the substrates, including proliferation, cell signaling pathways, and cell differentiation [38]. Initially, we examined NHDFs' morphology on each PMCxA substrate at 24 h. To visualize adhered NHDFs, they were stained using a calcein reagent, as shown in Figure 2a. Most of the adhered NHDFs on every substrate showed green fluorescence signals attributed to living cells. The cells were found to spread on uncoated PET substrate as well as on PMC4A, PMC5A, and PMC6A-coated substrates after 24 h of culture. In contrast, on the PMC2A- and PMC3A-coated substrates, cells retained their circular shape. In addition, the number of adhered cells on PMCxA substrates at a predetermined time was measured using the colorimetric WST-8 assay, as shown in Figure 2b. Over 60% of the initially seeded cells adhered to the uncoated PET, PMC4A, PMC5A, and PMC6A-coated substrates within 24 h. The number of adhered cells on the PMC4A was approximately 76% of initially seeded cells and the highest among all substrates. The PMC2A and PMC3A significantly reduced the number of attached cells compared to other substrates. After 96 h and 168 h of incubation, the number of cells on the substrates decreased in the following order: PMC4A > PMC6A > PMC5A > PET > PMC3A > PMC2A. Although there was an almost two-fold increase in the number of adhered cells on all substrates at 96 h, it showed a five-fold and a seven-fold increase on PMC2A and PMC4A at 196 h, respectively. Therefore, the proliferation of cells on PMC2A was significantly lower than that on PET and other substrates at all time intervals, while the proliferation of cells on PMC4A was significantly higher than that of other substrates.

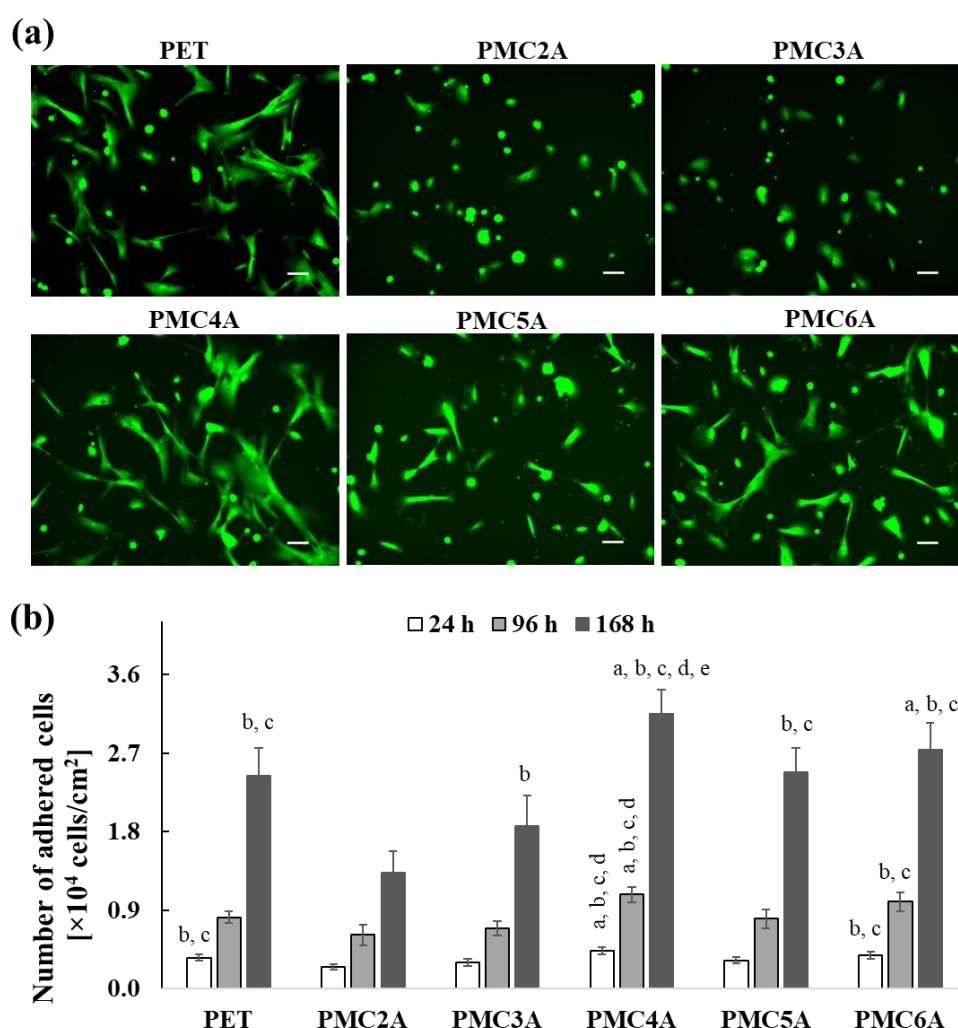


Figure 2. (a) Calcein staining images for NHDFs adhered on PET, PMC2A, PMC3A, PMC4A, PMC5A, and PMC6A after 24 h of incubation (scale bars = 100 μm). (b) The number of adhered NHDF on PMCx-coated substrates at 24, 96, and 168 h. The data represent the mean \pm SD ($n = 3$, ^a $p < 0.05$ compared with PET, ^b $p < 0.05$ compared with PMC2A, ^c $p < 0.05$ compared with PMC3A, ^d $p < 0.05$ compared with PMC5A, ^e $p < 0.05$ compared with PMC6A; Tukey's multiple comparisons test).

Guerra et al. reported that the stiffness of the substrate has an impact on cellular behavior [39]. In their study, MC3T3-E1 cells were cultured on substrates coated with poly(*n*-alkyl acrylate)s with various lengths of side-chain alkyl groups with different mechanical stiffnesses. The substrate stiffness declined linearly with an increasing side chain alkyl length, leading to better cellular interactions on the stiffer substrate compared to the flexible substrate. In our results, we found that the cell adhesion and proliferation of NHDFs were modulated on the substrates coated with PMCxAs, of which the chemical structures were similar to the methoxy groups at the side chains. This suggests that the mechanical stiffness of substrates based on the side chain of PMCxAs might be one of the factors affecting cell adhesion and proliferation, although the stiffness of the surface of PMCx coatings has not been measured in the present study. However, PMC4A exhibited excellent cell adhesion behavior and proliferation (Figure 2a). The physicochemical properties, such as wettability, surface energy, the balance of hydrophilicity and hydrophobicity, roughness, polymer chain mobility, chemical functionalities, and hydration water content, are known to affect cell behavior [16,40]. Since PMCx altered these properties, the cells adhered to the PMCxAs would be influenced by the balance of the hydrophilicity and hydrophobicity of polymers, and the hydration water content of polymers.

3.3. Quantification of Adsorbed Protein on Polymer Substrates

The amount and conformational changes of adsorbed proteins, such as FN and vitronectin, are another important factor that may be involved in the cell attachment process [41,42]. The amount of adsorbed FN on the substrates is likely to affect NHDFs' adhesion. Therefore, the amount of adsorbed FN on the PMCxA-coated substrate was analyzed, as shown in Figure 3. The amount of adsorbed FN on the substrates increased with an increase in the carbon length up to PMC4A but decreased for PMC5A and PMC6A compared to PMC4A. The amount of adsorbed FN on PMC2A was significantly lower, while that on PMC4A was significantly higher than that on PET and other substrates, except for PMC6A. Considering the number of adhered NHDFs on the PMCxA substrates, the adsorbed FN on PMC4A enhanced the adhesion and proliferation of NHDFs, whereas PMC2A suppressed NHDFs' adhesion. Our group has previously clarified that the presence of IW within or on the hydrated polymer surface acts as a repulsive barrier between the proteins and the substrate, leading to poor interactions between them [9,10]. A previous study on a PMEA analog PMCxA-coated substrate demonstrated that the amount of adsorbed fibrinogen increased as the side chain increased, implying that hydrophobicity was an essential factor [33]. Moreover, another study indicated that the enhancement of the adsorbed protein layer was correlated with the mobility of the polymer surface [37]. Therefore, the FN adsorption was also modulated by hydration water, the balance of hydrophilicity and hydrophobicity, and polymer mobility.

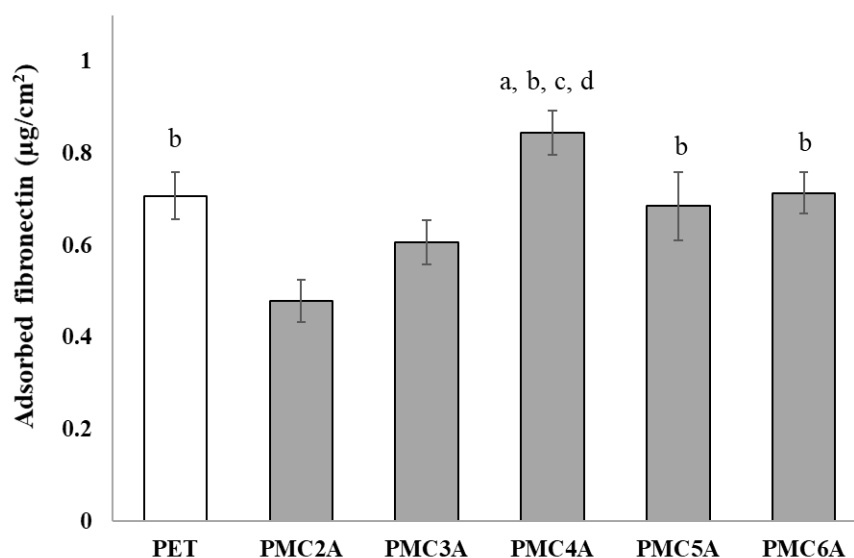


Figure 3. Evaluation of adsorbed fibronectin on substrates coated with PMCxAs. The data represent the mean \pm SD ($n = 15$, ^a $p < 0.05$ compared with PET, ^b $p < 0.05$ compared with PMC2A, ^c $p < 0.05$ compared with PMC3A, ^d $p < 0.05$ compared with PMC5A; Tukey's multiple comparisons test).

3.4. Immunocytochemical Assay

The physicochemical properties and adsorbed proteins on the biomaterial surface affect cell adhesion behavior, cell signaling pathways, and cell differentiation. Focal adhesion plays a crucial role in transmitting mechanochemical signals, together with integrin clusters, providing strength between integrin and actin connections, and is a crucial factor in tissue regeneration, maintenance, and repair via cell signaling for direct cell migration, proliferation, and differentiation [43]. Therefore, cell morphology and the formation of focal adhesions in cells are initial indicators of cell signaling pathways with cell adhesion on biomaterial surfaces. Immunocytochemical assays for F-actin and vinculin were conducted to evaluate the cellular functions of adhered NHDFs on the substrates (Figure 4a). Focal adhesions were identified via the localization of actin filaments and vinculin [44]. NHDFs were found to be entirely spread on PET, and several focal adhesions in the cells were

observed on the PET through the thicker extension of actin filaments and the observation of vinculin localization at the tip of actin filaments as a dot. However, on the PMC2A- and PMC3A-coated substrates, actin, and vinculin were not fully developed, suggesting that very few focal adhesions were observed on PMC2A and PMC3A. Although the shape of the NHDFs showed spreading on PMC4A, PMC5A, and PMC6A, focal adhesion with denser actin filament extension and vinculin localization was significant on the NHDFs adhered to PMC4A compared to those on PMC5A and PMC6A. In addition, the cells adhered to a coated substrate of PMCxAs were calculated using confocal images for various parameters, including area, circularity, and aspect ratio (Figure 4b–d). The round shape of the cells was observed on PMC2A- and PMC3A-coated substrates because of the limited spreading area, high circularity, and low aspect ratio. Contrasting results, such as a larger spreading area, a low circularity, and a higher aspect ratio, were observed on the PMC4A-coated substrate. Typically, focal adhesions are known to occur through interactions between integrin and ECM proteins [45,46]. In our previous reports, protein adsorption has already been shown to be suppressed on PMEA analog-coated surfaces compared with tissue culture polystyrene (TCPS) [25,32]. Hence, because of the adsorption of a limited amount of ECM proteins, focal adhesion formation was suppressed on PMC2A- and PMC3A-coated substrates. In contrast, the strong focal adhesion of cells on the PMC4A-coated substrate was attributed to the higher amount of adsorbed FN (Figure 3).

3.5. Immunoblotting Studies

The adhesion of fibroblasts onto biomaterial surfaces is generally carried out through the interaction between $\alpha 5\beta 1$ or $\alpha v\beta 3$ integrins and the cell-binding motif of adhesive proteins [9,19]. Integrin signaling in fibroblasts is related not only to cell adhesion and proliferation but also to fibroblast differentiation. Fibroblasts differentiate into α -SMA-expressing myofibroblasts [47]. As a marker of fibroblast-to-myofibroblast differentiation, the expression of α -SMA has already been recognized, the differentiation of which plays a vital role in accelerating wound repair [21,48]. Snail and vimentin expression is also associated with fibroblast differentiation and proliferation [49,50]. To further clarify the cell behavior on the PMCxAs, we measured the differential expression of cytoskeletal proteins, which could be a phenotypic marker of myofibroblasts, such as Snail, α -SMA, and vimentin, by immunoblotting (Figure 5). The ratio of band strength was calculated to assess the expression levels of proteins in cells (Figure 5b–d). Snail, α -SMA, and vimentin were more highly expressed in cells cultured on the PMC4A-coated substrate than in those cultured on other substrates. These results indicate that a robust integrin-dependent interaction between PMC4A and NHDF may induce myofibroblast differentiation. The function of FN in controlling cellular adhesion, migration, and differentiation has already been reported [42].

3.6. Cell Migration Test

The modulation of fibroblast-to-myofibroblast differentiation and fibroblast migration is essential for the development of wound dressing materials [51]. Cell migration is the directionality of cells migrating toward the wounded area. To evaluate whether PMCxA substrates could be utilized in wound healing, a migration test was performed using the scratch procedure. The migration of NHDFs, migration area, and healing rate in the wound region are shown in Figure 6a–c, respectively. Figure 6a shows that the area of the scratch was significant at 0 h, while the region decreased from 0 to 24 and 48 h. The migration area was found to increase over time (Figure 6b), which implies the migration of cells towards the wound via autocrine or paracrine mechanisms [51]. Figure 6c also shows that the migration rate of cells on the substrate coated with PMC2A (4.81 $\mu\text{m}/\text{h}$; slope from Figure 6b and PMC3A (5.72 $\mu\text{m}/\text{h}$) was lower than that on the other substrates. It is crucial that the cells on PMC4A substrates migrate rapidly to the scratched area, resulting in a rapid decline in the area (12.47 $\mu\text{m}/\text{h}$). For PMC5A- and PMC6A-coated substrates, cells also migrated to the scratched area. Although the migration rate was lower than that on PMC4A, the

differences were not significant compared with those on PET and other substrates. The fibroblast-to-myofibroblast differentiation is attributed to the expression of a phenotypic marker of myofibroblasts and the increase in the migration of cells [49,50]. Therefore, it suggested that the increase in the migration of NHDFs on PMC4A was accompanied by the fibroblast-to-myofibroblast differentiation, whereas PMC2A suppressed the migration of NHDFs and the differentiation.

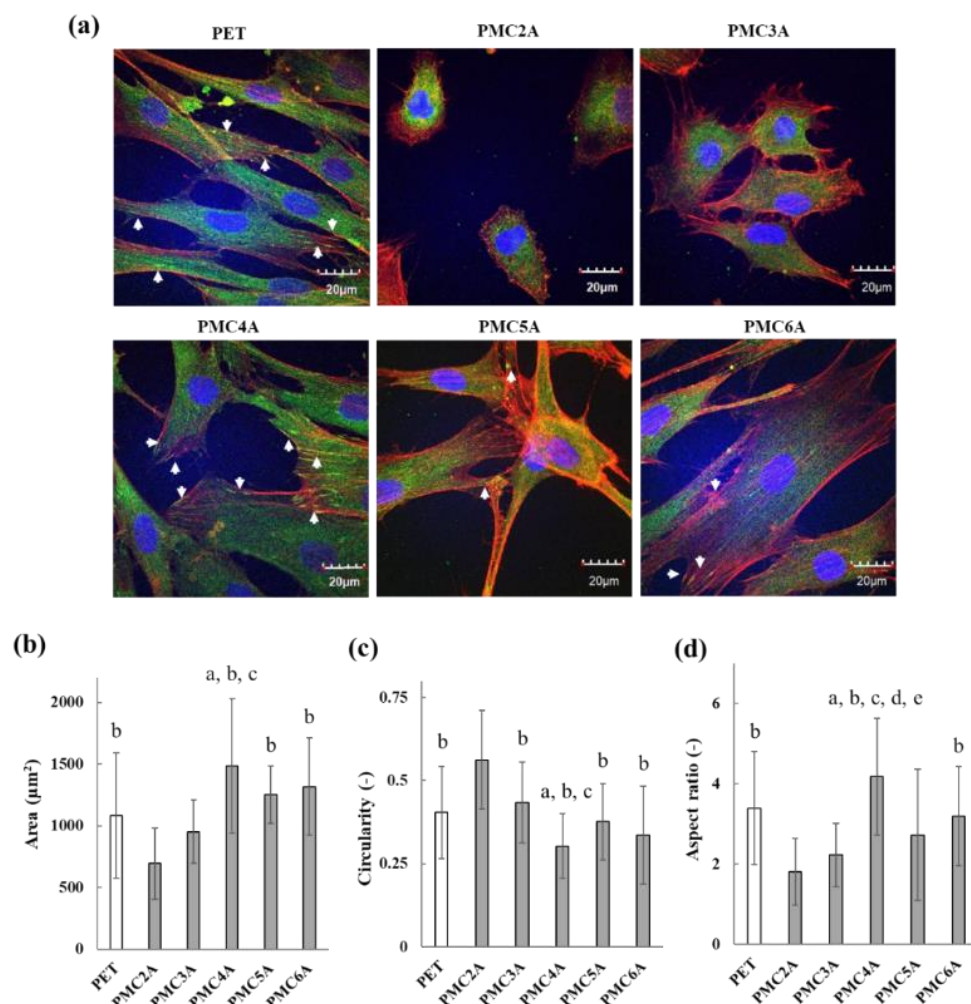


Figure 4. (a) CLSM photos of PMCxA-coated substrates for focal adhesion formation. Blue: cell nuclei; green: vinculin; red: actin fibers. Arrows indicate focal adhesion. Cell morphologies were determined by (b) spreading area, (c) circularity, and (d) aspect ratios of NHDFs on PMCxA-coated substrates calculated from CLSM images. The data represent the mean \pm SD ($n = 15$, ^a $p < 0.05$ compared with PET, ^b $p < 0.05$ compared with PMC2A, ^c $p < 0.05$ compared with PMC3A, ^d $p < 0.05$ compared with PMC5A, ^e $p < 0.05$ compared with PMC6A; Tukey's multiple comparisons test). Each experiment was carried out at least three times.

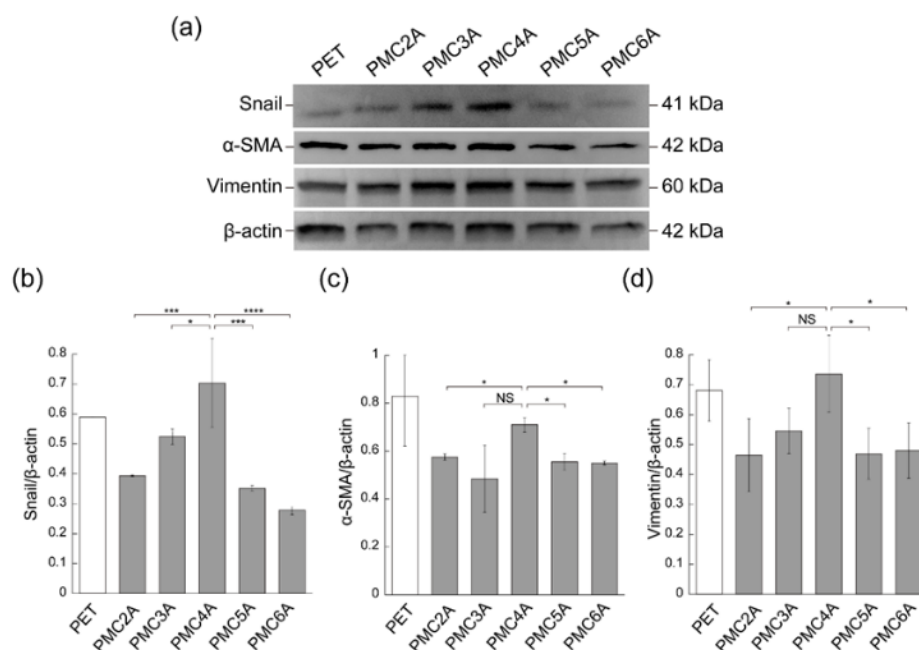


Figure 5. (a) Immunoblotting analysis for Snail, α-SMA, vimentin, and β-actin in NHDF cultured on PET, PMC2A, PMC3A, PMC4A, PMC5A, and PMC6A. (b–d) The band intensity for (b) Snail/β-actin, (c) α-SMA/β-actin, and (d) vimentin/β-actin ($n = 3$, * $p < 0.05$, *** $p < 0.001$, **** $p < 0.0001$; Tukey's multiple comparisons test).

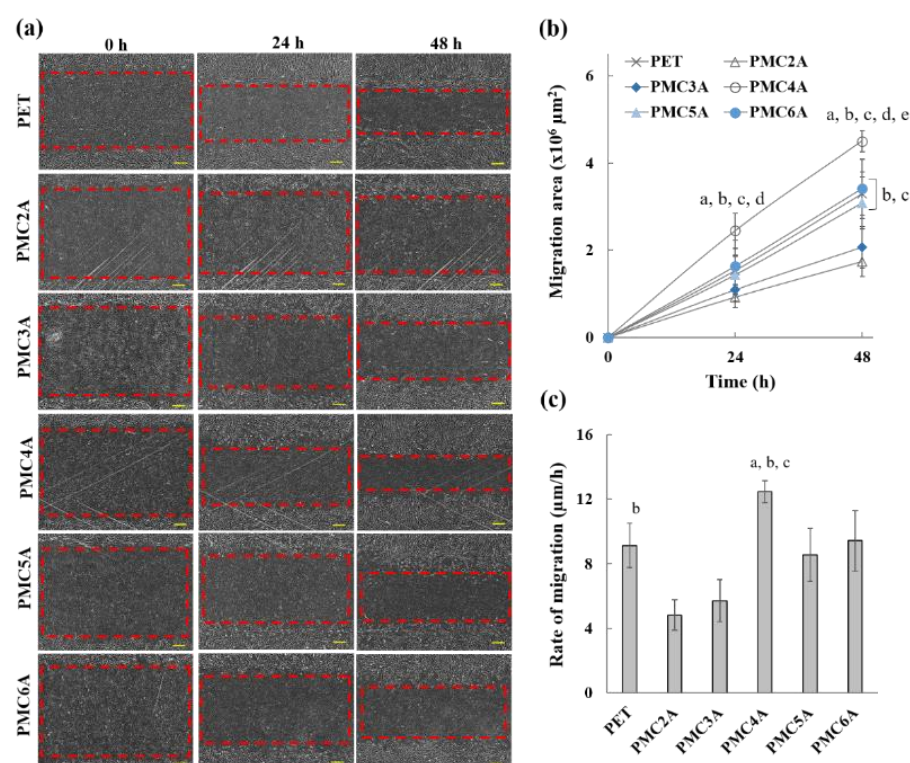


Figure 6. (a) Microscopic images of cell migration of NHDFs, (b) migration area, and (c) rate of migration on PMC_xA-coated substrates (scale bar = 300 μm). The data represent the mean ± SD ($n = 5$, ^a $p < 0.05$ compared with PET, ^b $p < 0.05$ compared with PMC2A, ^c $p < 0.05$ compared with PMC3A, ^d $p < 0.05$ compared with PMC5A, ^e $p < 0.05$ compared with PMC6A; Tukey's multiple comparisons test).

3.7. Total Collagen Measurement

In wound healing, the function of collagen is associated with the attraction of fibroblasts and the secretion of new collagen at the injured location [52]. To verify the possibility of wound healing, it is important to determine whether the secretion of collagen from NHDFs is promoted on PMCA-coated substrates. In this experiment, a comparatively higher density of NHDFs was plated on PMCA-coated substrates to prevent proliferation and accelerate collagen growth. The concentration of secreted collagen from the cells was measured (Figure 7). Collagen secretion was significantly higher for substrates coated with PMC4A than for other substrates. Collagen secretion for PMC5A- and PMC6A-coated substrates was similar to that for PET. For PMC2A, however, a significantly lower collagen output was observed in NHDFs. Hence, it suggested PMC4A could recruit the fibroblast which secreted a large amount of collagen while the secretion of collagen from fibroblast was reduced by PMC2A. The regulation of the amount of collagen plays an important role in restoring the strength and function of wound tissue [52]. PMCA may be utilized in the wound healing process to adjust the amount of collagen to be suitable for the tissue.

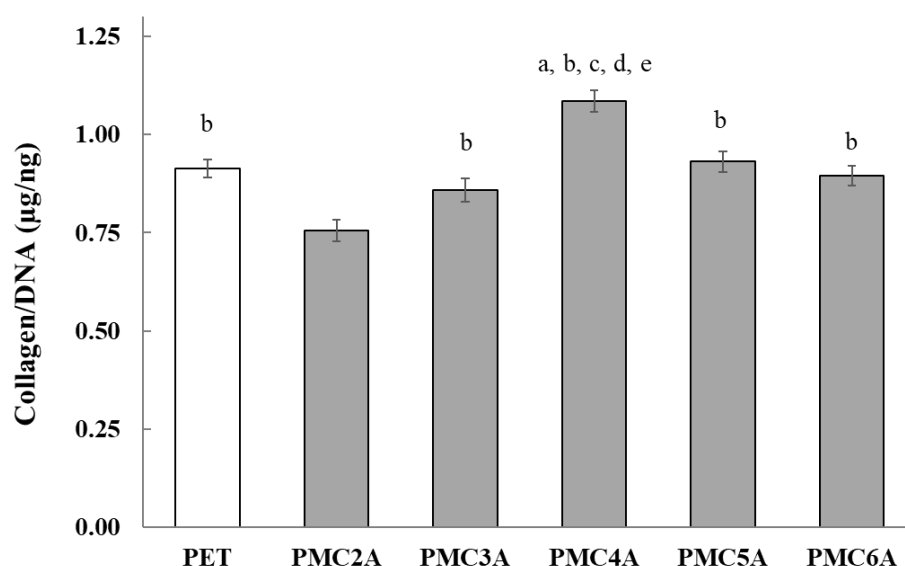


Figure 7. Total soluble collagen production by NHDFs on PMCA substrates. The data represent the mean \pm SD ($n = 5$, ^a $p < 0.05$ compared with PET, ^b $p < 0.05$ compared with PMC2A, ^c $p < 0.05$ compared with PMC3A, ^d $p < 0.05$ compared with PMC5A, ^e $p < 0.05$ compared with PMC6A; Tukey's multiple comparisons test).

In the present study, we revealed that PMC4A enhanced fibroblast-to-myofibroblast differentiation, cell migration, and collagen synthesis and secretion in adhered NHDFs, while PMC2A suppressed these functions in the cells. PMCA were polymers whose properties, such as hydrophobicity, T_g , and hydration water content, were modulated systematically with the change in the number of methylene carbons on the side chain. Several studies have reported that cell migration, proliferation, and differentiation are influenced by physicochemical properties such as stiffness and hydration water content on the substrates. Engler et al. demonstrated that mesenchymal stem cells migrated to stiffer regions on hydrogels with different degrees of stiffness, known as durotaxis [53,54]. Han et al. reported that vascular smooth muscle cells were perceived to migrate towards the low hydration side of poly(sodium 4-styrenesulfonate)/poly(diallyl dimethylammonium) chloride multilayers with swelling differences [55]. Evans et al. reported that cells can sense underlying stiff material through a soft layer at low ($<10 \mu\text{m}$) thickness [56]. Because the thickness of the PMEA derivative polymer-coated layer, which was coated by almost the same procedure as used in the present study on the PET substrates and was determined to be around 80 nm, the effect of stiffness attributed to the PMCA layer would not be

predominant, but that of PET was [57]. Therefore, hydration water content, hydrophobicity, and mobility of PMCxAs might affect the NHDFs' behavior. We summarized the behavior of NHDFs adhered to the PMCxAs as shown in Figure 8. By changing the number of methylene carbons, PMCxAs-coating modulated the amount of adsorbed fibronectin, hydrophobicity, and hydration water content on the substrates, leading to the change in NHDFs' behavior. However, the cell behavior did not change with the increasing number of methylene carbons of PMCxAs, resulting in PMC4A bearing the intermediate properties among PMCxAs' significantly activated fibroblast behavior. Therefore, it suggested that there was an optimal value of parameters of polymer to activate the cells. The detailed mechanism of activation of cells by PMCxAs requires further investigation.

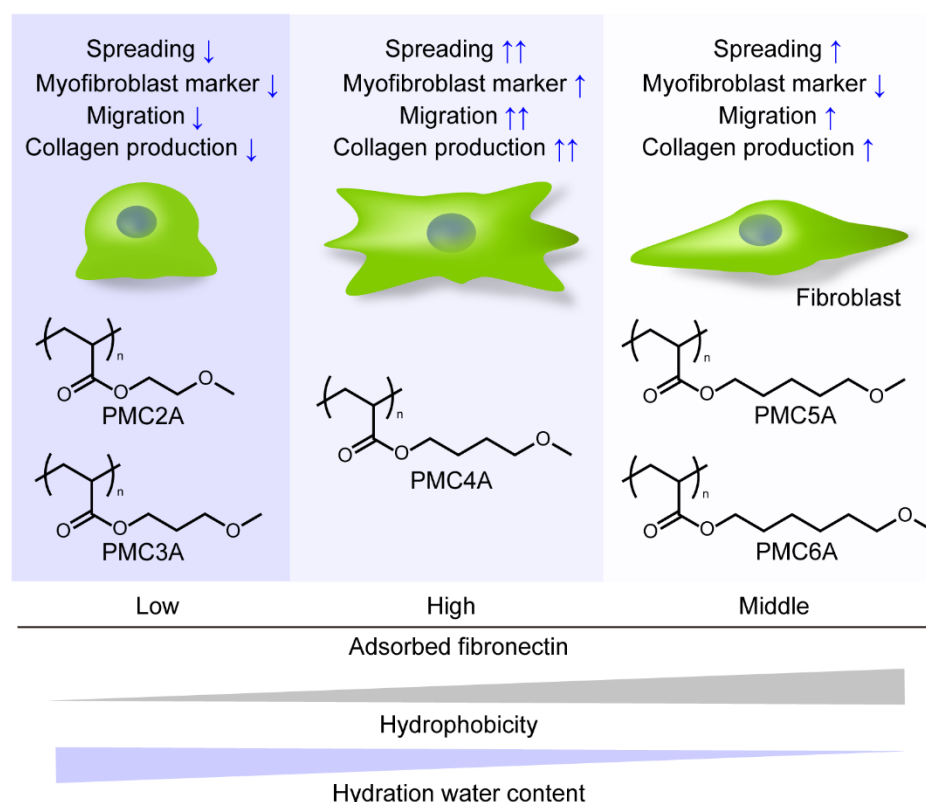


Figure 8. Schematic drawing of cellular behavior on PMCxAs-coated substrates.

The required function of wound healing materials is different for wound type, phase, and size [58]. In this regard, PMCxAs could tune the fibroblast behavior such as fibroblast-to-myofibroblast differentiation, cell migration, and collagen synthesis and secretion with the number of methylene carbon on the side chain. Hence, PMCxAs are anticipated to be successful materials for use in wound healing, with the ability to modulate cellular function.

4. Conclusions

One aspect of modern medical treatment is the control of cellular behavior, including adhesion, recruitment, and differentiation on the implant surface to avoid biological rejection and accelerate tissue repair. Fibroblast cells have a variety of functions that are mainly involved in the secretion of several cytokines and matrix proteins in the regulation of the immune response and tissue regeneration [10]. Differentiated myofibroblasts from fibroblasts induce the production of matrix proteins that allow dermal regeneration [11]. In the present study, PMEA analog polymers (PMCxAs) were chosen as coating materials to control the cell adhesion and growth behavior of fibroblasts, as the series of polymers modulate hydrophobicity, hydration water content, and protein adsorption by increasing the number of methylene groups in the side chain. As a result, PMC4A coating was found to

induce a greater spreading of cells, protein adsorption, focal adhesion formation, migration, expression of α -SMA on NHDFs, and collagen production. By contrast, the activation of NHDF adhered to PMC2A was lower than that adhered to other PMCxAs. According to the analysis of fibroblast behavior regulation, PMCxAs show promise as coating materials for biomaterials, such as biodegradable mesh-like materials for applications in wound healing.

Author Contributions: Conceptualization: T.A. and K.N.; methodology: R.A., K.N., H.M., S.K., T.A. and M.T.; formal analysis: R.A., K.N. and T.A.; investigation: R.A., K.N., H.M., S.K. and T.A.; data curation: R.A., K.N., T.A. and M.T.; writing—original draft preparation: R.A., K.N., T.A. and M.T.; writing—review and editing: R.A., K.N., D.M., S.K., T.A. and M.T.; visualization: R.A., K.N. and T.A.; supervision: T.A. and M.T.; project administration: M.T.; funding acquisition: M.T. All authors have read and agreed to the published version of the manuscript.

Funding: This study was funded by the Japan Society for the Promotion of Science (JSPS) (19H05720) from the Ministry of Education, Culture, Sports, Science, and Technology of Japan.

Institutional Review Board Statement: Not applicable.

Informed Consent Statement: Not applicable.

Data Availability Statement: The data presented in this study are available on request from the corresponding author.

Acknowledgments: We thank the Government of Japan (MEXT) for providing the scholarship for conducting a higher study and research at Kyushu University. We also thank the Cooperative Research Program “Dynamic Alliance for Open Innovation Bridging Human, Environment and Materials”.

Conflicts of Interest: The authors declare no conflict of interest.

References

- Schindhelm, K.; Milthorpe, B.K. Overview of biomaterials. *Australas. Phys. Eng. Sci. Med.* **1986**, *9*, 29–32. [[CrossRef](#)] [[PubMed](#)]
- Teo, A.J.; Mishra, A.; Park, I.; Kim, Y.J.; Park, W.T.; Yoon, Y.J. Polymeric biomaterials for medical implants and devices. *ACS Biomater. Sci. Eng.* **2016**, *2*, 454–472. [[CrossRef](#)]
- Saini, M. Implant biomaterials: A comprehensive review. *World J. Clin. Cases* **2015**, *3*, 52–57. [[CrossRef](#)]
- Ou, S.F.; Chen, C.S.; Hosseinkhani, H.; Yu, C.H.; Shen, Y.D.; Ou, K.L. Surface properties of nano-structural silicon-doped carbon films for biomedical applications. *Int. J. Nanotechnol.* **2013**, *10*, 945–958. [[CrossRef](#)]
- Chen, H.; Yuan, L.; Song, W.; Wu, Z.; Li, D. Biocompatible polymer materials: Role of protein-surface interactions. *Prog. Polym. Sci.* **2008**, *33*, 1059–1087. [[CrossRef](#)]
- Rahmati, M.; Silva, E.A.; Reseland, J.E.; Heyward, C.A.; Haugen, H.J. Biological responses to physicochemical properties of biomaterial surface. *Chem. Soc. Rev.* **2020**, *49*, 5178–5224. [[CrossRef](#)]
- Cai, S.; Wu, C.; Yang, W.; Liang, W.; Yu, H.; Liu, L. Recent advance in surface modification for regulating cell adhesion and behaviors. *Nanotechnol. Rev.* **2020**, *9*, 971–989. [[CrossRef](#)]
- Wong, T.; McGrath, J.A.; Navsaria, H. The role of fibroblasts in tissue engineering and regeneration. *Br. J. Dermatol.* **2007**, *156*, 1149–1155. [[CrossRef](#)]
- Sriram, G.; Bigliardi, P.L.; Bigliardi-Qi, M. Fibroblast heterogeneity and its implications for engineering organotypic skin models in vitro. *Eur. J. Cell Biol.* **2015**, *94*, 483–512. [[CrossRef](#)] [[PubMed](#)]
- Ko, U.H.; Choi, J.; Choung, J.; Moon, S.; Shin, J.H. Physicochemically tuned myofibroblasts for wound healing strategy. *Sci. Rep.* **2019**, *9*, 16070. [[CrossRef](#)]
- Mori, L.; Bellini, A.; Stacey, M.A.; Schmidt, M.; Mattoli, S. Fibrocytes contribute to the myofibroblast population in wounded skin and originate from the bone marrow. *Exp. Cell Res.* **2005**, *304*, 81–90. [[CrossRef](#)]
- Bharath Rao, K.; Malathi, N.; Narashiman, S.; Rajan, S.T. Evaluation of myofibroblasts by expression of alpha smooth muscle actin: A marker in fibrosis, dysplasia and carcinoma. *J. Clin. Diagn. Res.* **2014**, *8*, 14–17. [[CrossRef](#)]
- Honda, E.; Park, A.M.; Yoshida, K.; Tabuchi, M.; Munakata, H. Myofibroblasts: Biochemical and proteomic approaches to fibrosis. *Tohoku J. Exp. Med.* **2013**, *230*, 67–73. [[CrossRef](#)] [[PubMed](#)]
- Witherell, C.E.; Abeyayehu, D.; Barker, T.H.; Spiller, K.L. Macrophage and fibroblast interactions in biomaterial-mediated fibrosis. *Adv. Healthc. Mater.* **2019**, *8*, 1–35. [[CrossRef](#)] [[PubMed](#)]
- Kerch, G. Polymer hydration and stiffness at biointerfaces and related cellular processes. *Nanomed. Nanotechnol. Biol. Med.* **2018**, *14*, 13–25. [[CrossRef](#)] [[PubMed](#)]
- Chen, L.; Yan, C.; Zheng, Z. Functional polymer surfaces for controlling cell behaviors. *Mater. Today* **2018**, *21*, 38–59. [[CrossRef](#)]

17. Bacakova, L.; Filova, E.; Parizek, M.; Ruml, T.; Svorcik, V. Modulation of cell adhesion, proliferation and differentiation on materials designed for body implants. *Biotechnol. Adv.* **2011**, *29*, 739–767. [\[CrossRef\]](#)
18. Wang, X.; Hu, X.; Dulinska-Molak, I.; Kawazoe, N.; Yang, Y.; Chen, G. Discriminating the independent influence of cell adhesion and spreading area on stem cell fate determination using micropatterned surfaces. *Sci. Rep.* **2016**, *6*, 28708. [\[CrossRef\]](#) [\[PubMed\]](#)
19. Wozniak, M.A.; Modzelewska, K.; Kwong, L.; Keely, P.J. Focal adhesion regulation of cell behavior. *Biochim. Biophys. Acta Mol. Cell Res.* **2004**, *1692*, 103–119. [\[CrossRef\]](#)
20. Wysotzki, P.; Gimsa, J. Surface coatings modulate the differences in the adhesion forces of eukaryotic and prokaryotic cells as detected by single cell force microscopy. *Int. J. Biomater.* **2019**, *2019*, 7024259. [\[CrossRef\]](#)
21. Nedela, O.; Slepicka, P.; Švorcik, V. Surface modification of polymer substrates for biomedical applications. *Materials* **2017**, *10*, 1115. [\[CrossRef\]](#)
22. Ye, Z.; Hiroyasu, K.; Yuya, S.; Kano, M.; Tada-Aki, K.; Shimizu, Y. MPC polymer regulates fibrous tissue formation by modulating cell adhesion to the biomaterial surface. *Dent. Mater. J.* **2010**, *29*, 518–528. [\[CrossRef\]](#)
23. Tanaka, M.; Motomura, T.; Kawada, M.; Anzai, T.; Kasori, Y.; Shiroya, T.; Shimura, K.; Onishi, M.; Mochizuki, A. Blood compatible aspects of poly(2-methoxyethylacrylate) (PMEA)-relationship between protein adsorption and platelet adhesion on PMEA surface. *Biomaterials* **2000**, *21*, 1471–1481. [\[CrossRef\]](#)
24. Hoshiba, T.; Nikaido, M.; Tanaka, M. Characterization of the attachment mechanisms of tissue-derived cell lines to blood-compatible polymers. *Adv. Healthc. Mater.* **2014**, *3*, 775–784. [\[CrossRef\]](#)
25. Hoshiba, T.; Nemoto, E.; Sato, K.; Orui, T.; Otaki, T.; Yoshihiro, A.; Tanaka, M. Regulation of the contribution of integrin to Cell attachment on poly(2-methoxyethyl acrylate) (PMEA) analogous polymers for attachment-based cell enrichment. *PLoS ONE* **2015**, *10*, e0136066. [\[CrossRef\]](#) [\[PubMed\]](#)
26. Tanaka, M.; Hayashi, T.; Morita, S. The roles of water molecules at the biointerface of medical polymers. *Polym. J.* **2013**, *45*, 701–710. [\[CrossRef\]](#)
27. Miwa, Y.; Ishida, H.; Saitô, H.; Tanaka, M.; Mochizuki, A. Network structures and dynamics of dry and swollen poly(acrylate)s. Characterization of high- and low-frequency motions as revealed by suppressed or recovered intensities (SRI) analysis of ¹³C NMR. *Polymer* **2009**, *50*, 6091–6099. [\[CrossRef\]](#)
28. Morita, S.; Tanaka, M.; Ozaki, Y. Time-resolved in situ ATR-IR observations of the process of sorption of water into a poly(2-methoxyethyl acrylate) film. *Langmuir* **2007**, *23*, 3750–3761. [\[CrossRef\]](#) [\[PubMed\]](#)
29. Tanaka, M.; Mochizuki, A. Effect of water structure on blood compatibility—Thermal analysis of water in poly(meth)acrylate. *J. Biomed. Mater. Res. Part A* **2004**, *68*, 684–695. [\[CrossRef\]](#)
30. Tanaka, M.; Sato, K.; Kitakami, E.; Kobayashi, S.; Hoshiba, T.; Fukushima, K. Design of biocompatible and biodegradable polymers based on intermediate water concept. *Polym. J.* **2015**, *47*, 114–121. [\[CrossRef\]](#)
31. Tanaka, M.; Kobayashi, S.; Murakami, D.; Aratsu, F.; Kashiwazaki, A.; Hoshiba, T.; Fukushima, K. Design of polymeric biomaterials: The “Intermediate water concept.”. *Bull. Chem. Soc. Jpn.* **2019**, *92*, 2043–2057. [\[CrossRef\]](#)
32. Hoshiba, T.; Nemoto, E.; Sato, K.; Maruyama, H.; Endo, C.; Tanaka, M. Promotion of adipogenesis of 3T3-L1 cells on protein adsorption-suppressing poly(2-methoxyethyl acrylate) analogs. *Biomacromolecules* **2016**, *17*, 3808–3815. [\[CrossRef\]](#)
33. Kobayashi, S.; Wakui, M.; Iwata, Y.; Tanaka, M. Poly(ω -methoxyalkyl acrylate)s: Nonthrombogenic polymer family with tunable protein adsorption. *Biomacromolecules* **2017**, *18*, 4214–4223. [\[CrossRef\]](#) [\[PubMed\]](#)
34. Jonkman, J.E.; Cathcart, J.A.; Xu, F.; Bartolini, M.E.; Amon, J.E.; Stevens, K.M.; Colarusso, P. An introduction to the wound healing assay using live-cell microscopy. *Cell Adhes. Migr.* **2014**, *8*, 440–451. [\[CrossRef\]](#) [\[PubMed\]](#)
35. Kumar, P.; Satyam, A.; Fan, X.; Collin, E.; Rochev, Y.; Rodriguez, B.J.; Gorelov, A.; Dillon, S.; Joshi, L.; Raghunath, M.; et al. Macromolecularly crowded in vitro microenvironments accelerate the production of extracellular matrix-rich supramolecular assemblies. *Sci. Rep.* **2015**, *5*, 8729. [\[CrossRef\]](#) [\[PubMed\]](#)
36. Bachhuka, A.; Hayball, J.; Smith, L.E.; Vasilev, K. Effect of surface chemical functionalities on collagen deposition by primary human dermal fibroblasts. *ACS Appl. Mater. Interfaces* **2015**, *7*, 23767–23775. [\[CrossRef\]](#)
37. Bathawab, F.; Bennett, M.; Cantini, M.; Reboud, J.; Dalby, M.J.; Salmerón-Sánchez, M. Lateral chain length in polyalkyl acrylates determines the mobility of fibronectin at the cell/material interface. *Langmuir* **2016**, *32*, 800–809. [\[CrossRef\]](#)
38. Xing, F.; Li, L.; Zhou, C.; Long, C.; Wu, L.; Lei, H.; Kong, Q.; Fan, Y.; Xiang, Z.; Zhang, X. Regulation and directing stem cell fate by tissue engineering functional microenvironments: Scaffold physical and chemical cues. *Stem Cells Int.* **2019**, *2019*, 2180925. [\[CrossRef\]](#)
39. Guerra, N.B.; González-García, C.; Llopis, V.; Rodríguez-Hernández, J.C.; Moratal, D.; Rico, P.; Salmerón-Sánchez, M. Subtle variations in polymer chemistry modulate substrate stiffness and fibronectin activity. *Soft Matter* **2010**, *6*, 4748–4755. [\[CrossRef\]](#)
40. Wong, J.Y.; Leach, J.B.; Brown, X.Q. Balance of chemistry, topography, and mechanics at the cell-biomaterial interface: Issues and challenges for assessing the role of substrate mechanics on cell response. *Surf. Sci.* **2004**, *570*, 119–133. [\[CrossRef\]](#)
41. Ngandu Mpoyi, E.; Cantini, M.; Reynolds, P.M.; Gadegaard, N.; Dalby, M.J.; Salmerón-Sánchez, M. Protein adsorption as a key mediator in the nanotopographical control of cell behavior. *ACS Nano* **2016**, *10*, 6638–6647. [\[CrossRef\]](#) [\[PubMed\]](#)
42. Parisi, L.; Toffoli, A.; Ghezzi, B.; Mozzoni, B.; Lumetti, S.; Macaluso, G.M. A glance on the role of fibronectin in controlling cell response at biomaterial interface. *Jpn. Dent. Sci. Rev.* **2020**, *56*, 50–55. [\[CrossRef\]](#) [\[PubMed\]](#)
43. Khalili, A.A.; Ahmad, M.R. A Review of cell adhesion studies for biomedical and biological applications. *Int. J. Mol. Sci.* **2015**, *16*, 18149–18184. [\[CrossRef\]](#)

44. Kanchanawong, P.; Shtengel, G.; Pasapera, A.M.; Ramko, E.B.; Davidson, M.W.; Hess, H.F.; Waterman, C.M. Nanoscale architecture of integrin-based cell adhesions. *Nature* **2010**, *468*, 580–584. [[CrossRef](#)] [[PubMed](#)]
45. Ziegler, W.H.; Liddington, R.C.; Critchley, D.R. The structure and regulation of vinculin. *Trends Cell Biol.* **2006**, *16*, 453–460. [[CrossRef](#)] [[PubMed](#)]
46. Gu, J.; Sumida, Y.; Sanzen, N.; Sekiguchi, K. Laminin-10/11 and fibronectin differentially regulate integrin-dependent Rho and Rac activation via p130Cas-CrkII-DOCK180 pathway. *J. Biol. Chem.* **2001**, *276*, 27090–27097. [[CrossRef](#)]
47. Hinz, B.; Celetta, G.; Tomasek, J.J.; Gabbiani, G.; Chaponnier, C. Alpha-smooth muscle actin expression upregulates fibroblast contractile activity. *Mol. Biol. Cell* **2001**, *12*, 2730–2741. [[CrossRef](#)]
48. Shinde, A.V.; Humeres, C.; Frangogiannis, N.G. The role of α -smooth muscle actin in fibroblast-mediated matrix contraction and remodeling. *Biochim. Biophys. Acta Mol. Basis Dis.* **2017**, *1863*, 298–309. [[CrossRef](#)]
49. Franz, M.; Spiegel, K.; Umbreit, C.; Richter, P.; Codina-Canet, C.; Berndt, A.; Altendorf-Hofmann, A.; Koscielny, S.; Hyckel, P.; Kosmehl, H.; et al. Expression of Snail is associated with myofibroblast phenotype development in oral squamous cell carcinoma. *Histochem. Cell Biol.* **2009**, *131*, 651–660. [[CrossRef](#)]
50. Cheng, F.; Shen, Y.; Mohanasundaram, P.; Lindström, M.; Ivaska, J.; Ny, T.; Erikss, J.E. Vimentin coordinates fibroblast proliferation and keratinocyte differentiation in wound healing via TGF- β -Slug signaling. *Proc. Natl. Acad. Sci. USA* **2016**, *113*, E4320–E4327. [[CrossRef](#)]
51. Tottoli, E.M.; Dorati, R.; Genta, I.; Chiesa, E.; Pisani, S.; Conti, B. Skin wound healing process and new emerging technologies for skin wound care and regeneration. *Pharmaceutics* **2020**, *12*, 735. [[CrossRef](#)]
52. Rangaraj, A.; Harding, K.; Leaper, D. Role of collagen in wound management. *Drug Invent. Today* **2020**, *13*, 55–57.
53. Kennedy, K.M.; Bhaw-Luximon, A.; Jhurry, D. Cell-matrix mechanical interaction in electrospun polymeric scaffolds for tissue engineering: Implications for scaffold design and performance. *Acta Biomater.* **2017**, *50*, 41–55. [[CrossRef](#)]
54. Tse, J.R.; Engler, A.J. Stiffness gradients mimicking in vivo tissue variation regulate mesenchymal stem cell fate. *PLoS ONE* **2011**, *6*, e15978. [[CrossRef](#)] [[PubMed](#)]
55. Han, L.; Mao, Z.; Wu, J.; Guo, Y.; Ren, T.; Gao, C. Directional cell migration through cell-cell interaction on polyelectrolyte multilayers with swelling gradients. *Biomaterials* **2013**, *34*, 975–984. [[CrossRef](#)] [[PubMed](#)]
56. Tusan, C.G.; Man, Y.H.; Zarkoob, H.; Johnston, D.A.; Andriotis, O.G.; Thurner, P.J.; Yang, S.; Sander, E.A.; Gentleman, E.; Sengers, B.G.; et al. Collective cell behavior in mechanosensing of substrate thickness. *Biophys. J.* **2018**, *114*, 2743–2755. [[CrossRef](#)] [[PubMed](#)]
57. Hoshiba, T.; Orui, T.; Endo, C.; Sato, K.; Yoshihiro, A.; Minagawa, Y.; Tanaka, M. Adhesion-based simple capture and recovery of circulating tumor cells using a blood-compatible and thermo-responsive polymer-coated substrate. *RSC Adv.* **2016**, *6*, 89103–89112. [[CrossRef](#)]
58. Okur, M.E.; Karantas, I.D.; Şenyiğit, Z.; Üstündağ Okur, N.; Siafaka, P.I. Recent trends on wound management: New therapeutic choices based on polymeric carriers. *Asian J. Pharm. Sci.* **2020**, *15*, 661–684. [[CrossRef](#)]